Journal of Applied and Computational Mechanics, Vol. 1, No. 1, (2015), 17-25
DOI: 10.22055/jacm.2014.10552

Journal of
Applied and Computational Mechanics

Pull-in behavior analysis of vibrating functionally graded micro-cantilevers under suddenly DC voltage

Jamal Zare

National Iranian South Oil Company (NISOC), Ahvaz, Iran

Received February 03 2014; revised June 06 2014; accepted for publication June 22 2014.
Corresponding author: jamal.zare@hotmail.com

Abstract

The present research attempts to explain dynamic pull-in instability of functionally graded micro-cantilevers actuated by step DC voltage while the fringing-field effect is taken into account in the vibrational equation of motion. By employing modern asymptotic approach namely Homotopy Perturbation Method with an auxiliary term, high-order frequency-amplitude relation is obtained. Then, the influences of material properties and actuation voltage on dynamic pull-in behavior are investigated. It is demonstrated that the auxiliary term in the homotopy perturbation method is extremely effective for higher order approximation and two terms in series expansions are sufficient to produce an acceptable solution. The strength of this analytical procedure is verified through numerical results.

Keywords: Micro-actuator, Functionally graded material, Dynamic Pull-in instability, Homotopy Perturbation Method with an auxiliary term.

1. Introduction

A Functionally Graded Material (FGM) is characterized by a gradual change in material properties over volume. It is an anisotropic composite material where a material gradient is deliberately introduced over two different materials. Research into the behaviour of functionally graded materials (FGMs) has been an interesting topic during the past decades [1, 2]. In recent years, FGMs find increasing applications in micro-structures, such as thin films in the form of shape memory alloys [3, 4] and micro-electro-mechanical systems (MEMS) [5-7]. FGMs are special composites whose composition varies continuously as a function of position along thickness of a structure to achieve an appropriate function. This is obtained by gradually varying volume fraction of the constituent materials. FGMs are generally made of a mixture of ceramic and metal to satisfy the demand of ultra-high-temperature environment and to eliminate the interface problems, as ceramic has a low thermal conductivity and thus excellent temperature residence [1]. Accordingly, the area of smart materials and structures has experienced rapid growth. The mechanics of smart structures involve coupling between the mechanical, electrical or thermal effects.

A non-conventional thin plate theory, coupled with the continuum surface elasticity model, has been developed by Lü et al. [2] for nano-scaled FGM films. They studied the effects of length scales, gradient index and aspect ratio on the displacements of FGM nano-plates. A size-dependent formulation for FGM Timoshenko beam on the basis of the modified couple stress theory has been proposed by Asghari et al. [8]. In addition, they obtained the closed-form analytic expressions for the bending and axial deformations and also the angle of rotation of the cross sections. Sadeghi-Pournaki et al. [9] presented the mechanical behaviour of functionally graded (FG) cantilever micro-beams subjected to a nonlinear electrostatic pressure and thermal moment considering effects of material length scale parameters. Ke and Wang [10] investigated the dynamic stability of microbeams made of functionally graded materials (FGMs) based on the modified couple stress theory and Timoshenko beam theory. They also discussed the influences of the length scale parameter, gradient index and length-to-thickness ratio on the dynamic stability characteristics of FGM microbeams with hinged–hinged and clamped–clamped end supports. Sharafkhani et al. [11] studied the mechanical behavior of a circular functionally graded material (FGM) micro-plate subjected to a nonlinear electrostatic pressure and mechanical shock and investigated the effects of different percentages of metal and ceramic constituent on the response of the system.

MEMS devices that integrate electrical and mechanical elements, because of their small size and weight, are widely used in inkjet printers, airbag deployment systems, automobile stability control systems, Digital Light Processing (DLP) technology, micro pumps, optical switches, micro-tweezers and micro-mirrors. Recently several numerical and experimental studies have been conducted on the pull-in instability and dynamic behavior of MEMS devices. In the dynamic analysis of micro-systems, electrostatic forces cause the relationship between the input excitation and the output response to be nonlinear. Pull-in and snap-through instabilities in transient deformations of microelectromechanical systems have been presented by Das and Batra [12]. They revealed that with a decrease in the rate of the applied potential difference, the pull-in and the snap-through parameters approach those for a static problem. Fu and Zhang [13] discussed the surface energies on the static and dynamic responses, pull-in voltage and pull-in time of electrically actuated nano beams by applying the Gurtin and Murdoch's theory of surface. They also included the effect of the geometrical nonlinearity in their study. Wang et al. [14] established the mathematical model to estimate the pull-in parameters and the fundamental frequency in a pre-stressed multi-layer microbeam with nonlinearities such as electro static loads and large deformation. Jia et al. [15] investigated the pull-in instability of micro-switches under the combined electrostatic and intermolecular forces and axial residual stress. They obtained pull-in voltage and pull-in deflection for micro-switches with four different boundary conditions using the differential quadrature method (DQM). Sedighi and Shirazi [16] presented a new asymptotic procedure to predict the nonlinear vibrational behavior of classical micro-beams pre-deformed by an electric field. They investigated the influences of basic parameters on pull-in instability and natural frequency of micro structures. Rahaeifard et al. [17] studied the dynamic behavior of microcantilevers under suddenly applied DC voltage based on the modified couple stress theory. They employed multiple scales method (MSM) and finite difference method to predict the dynamic behavior of the microbeams. Rajabi and Ramezani [18] developed a micro scale nonlinear beam model based on strain gradient elasticity. Towfighian et al. [19] presented the closed-loop dynamics of a chaotic electrostatic microbeam actuator and plotted the bifurcation diagrams which obtained by sweeping the AC voltage amplitudes and frequency.

Studying the asymptotic analysis of nonlinear problems has been rapidly developed more recently. Several researchers employed analytic approaches such as Max-Min approach [20], Energy Balance Method [21], Variational Iteration Method [22], Homotopy Analysis Method [23], ADM-Padé technique [24], Optimal Homotopy Asymptotic Method [25], Parameter Expansion Method [26,27], Hamiltonian Approach (HA) [28] and Iteration Perturbation Method [29] to study the static and dynamic behavior of nonlinear systems. Recently an asymptotic approach namely Homotopy Perturbation Method (HPM) with and auxiliary term proposed by He [30] has proven to be a very effective and convenient method for solving nonlinear governing equations.

The present article intends to compute the second-order frequency amplitude relation of vibrating micro-actuators in order to investigate the dynamic pull-in phenomenon by considering the fringing-field effect. To this end, analytical expressions for vibrational response of FGM micro-actuators are presented. The obtained approximate solution demonstrates that two terms in series expansions are sufficient to obtain a highly accurate solution of vibrating micro-beams. Finally, the influences of vibration amplitude, actuation voltage and material properties on the pull-in instability and fundamental frequency are studied.

2. Governing equation of functionally graded micro-actuator

A typical model of a functionally graded micro-cantilever above a rigid plate is illustrated in Fig. 1. The micro-beam has length l, thickness h, width b and initial gap g which is under step DC actuation voltage V. The distance of any point of the micro-structure from the neutral axis and the top surface are denoted by z and $\tilde{z}$, respectively. Furthermore, the distance of the neutral axis from the top surface is represented by $\tilde{z}_1$ and the configuration of coordinate system is also indicated in Fig. 2. It is assumed that the FGM micro-beam property which is made of metal and ceramic phases, along its thickness can be expressed by the following formula [1]:

$$E\left(\tilde{z}\right) = E_1 + \left(\frac{\tilde{z}}{h}\right)^n \left(E_2 - E_1\right) \tag{1}$$

The governing equation of motion of vibrating micro-actuator assuming Euler-Bernoulli beam theory is expressed as follows:

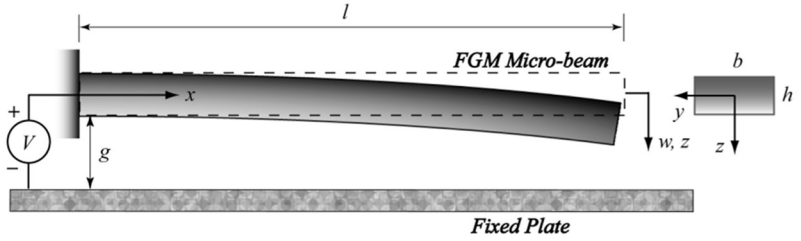

Fig. 1. Configuration of an actuated FGM micro-cantilever

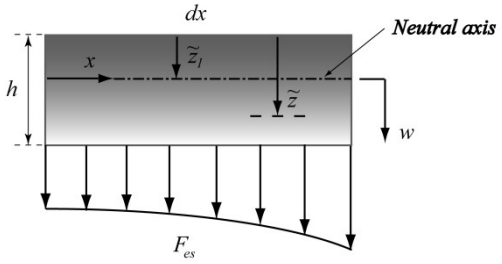

Fig. 2. Schematic representation of FGM micro-beam element

$$mw_{tt} + (EI)_{eq} w_{xxxx} - F_{es} = 0 \tag{2}$$

In which m is the mass per unit length of the beam and F_{es} denotes the electrostatic force. In order to describe the electrostatic actuation force, a more realistic situation including ‘‘fringing-field’’ modification field must be taken into consideration. The electrostatic force per unit length can be written as [31]:

$$F_{es} = \frac{1}{2}\frac{b\varepsilon V^2}{(g-w)^2}(1+f_f) \tag{3}$$

where $\varepsilon = 8.854187817620\times10^{-12}\ F/m$ is the vacuum permittivity and the parameter f_f represents the first order fringing-field correction and may be expressed as:

$$f_f = \beta_{es}\frac{g-w}{b} \tag{4}$$

In the aforementioned equation, the parameter β_{es} is set to 0.65 [31]. According to Asghari et al. [1], the effective flexural rigidity $(EI)_{eq}$ of FGM micro-beam can be expressed as:

$$(EI)_{eq} = \int_0^h (\tilde{z}-\tilde{z}_1)^2\left[E_1 + \left(\frac{\tilde{z}}{h}\right)^n (E_2-E_1)\right] b d\tilde{z} = bh^3 E_1 \tilde{\mu}(n) \tag{5}$$

where

$$\tilde{\mu}(n) = \frac{1}{3} + \frac{(\mu_{1-2}-1)}{n+3} + \left(1+\frac{\mu_{1-2}-1}{n+1}\right)\left(\frac{1+\frac{\mu_{1-2}-1}{n+2}}{1+\frac{\mu_{1-2}-1}{n+1}}\right)^2 - \left(\mu_{1-2}+2\frac{\mu_{1-2}-1}{n+2}\right)\frac{1+\frac{\mu_{1-2}-1}{n+2}}{1+\frac{\mu_{1-2}-1}{n+1}} \tag{6}$$

In equation (6), the parameter μ_{1-2} represents the ratio of metal to ceramic phases of micro-beam. By introducing the following non-dimensional variables:

$$\bar{\tau} = \sqrt{\frac{E_1 h^2}{\rho h l^4}}\,t,\ \ W = \frac{w}{g},\ \xi = \frac{x}{l},\ \ \bar{V}^2 = \frac{2\varepsilon l^4 V^2}{E_1 h^3 g^3},\ \ \alpha = \frac{g}{b} \tag{7}$$

the non-dimensional nonlinear governing equation of motion can be written as follows:

$$\frac{\partial^2 W}{\partial \bar{\tau}^2} + \tilde{\mu}(n)\frac{\partial^4 W}{\partial \xi^4} - \frac{\bar{V}^2}{(1-W)^2}\left(1+\alpha\beta_{es}(1-W)\right) = 0 \tag{8}$$

Using Taylor expansion for electrostatic force in equation (8) results in:

$$\frac{\partial^2 W}{\partial \tau^2} + \tilde{\mu}(n)\frac{\partial^4 W}{\partial \xi^4} - \frac{\bar{V}^2}{4}\sum_{n=0}^{\infty}(n+1+\alpha\beta_{es})W^n = 0 \tag{9}$$

Assuming $W(\xi,\tau) = q(\tau)\phi(\xi)$, where $\phi(\xi)$ is the first mode shape of micro-cantilever which can be expressed as:

$$\phi(\xi) = \cosh(\lambda\xi) - \cos(\lambda\xi) - \frac{\cosh(\lambda)+\cos(\lambda)}{\sinh(\lambda)+\sin(\lambda)}\left(\sinh(\lambda\xi)-\sin(\lambda\xi)\right) \tag{10}$$

where $\lambda = 1.875$ is the root of characteristic equation for first eigenmode. Applying the Bubnov-Galerkin method, the governing equation can be extracted as follows:

$$\ddot{q}(\bar{\tau}) + \gamma_1' q(\bar{\tau}) + \gamma_2'(q(\bar{\tau}))^2 + \gamma_3'(q(\bar{\tau}))^3 + \gamma_4'(q(\bar{\tau}))^4 + \gamma_0' = 0 \tag{11}$$

where

$$\gamma_1' = \gamma_1 + \tilde{\mu}(n)\lambda^4$$
$$\gamma_i' = \int_0^1 \gamma_i \phi^{i+1} d\xi, \ (i \neq 1) \tag{12}$$

3. Approximation by HPM with an auxiliary term

Consider a general nonlinear governing equation

$$L(q) + N(q) = 0 \tag{13}$$

where L and N are the linear and nonlinear operators, respectively. Recently, He [30] proposed the homotopy equation with an auxiliary term as follows:

$$\tilde{L}(q) + p\left(L(q) - \tilde{L}(q) + N(q)\right) + \alpha_1 p(1-p)q = 0 \tag{14}$$

where α_1 is an auxiliary parameter and $\tilde{L}$ is a linear operator with a possible unknown constant and $\tilde{L}(q) = 0$ can approximately describe the solution property. It should be pointed out that there is an alternative approach using the homotopy perturbation method by multiple homotopy parameters to solve nonlinear problems in which different nonlinear terms exist in the governing equation (see He [32]). In the nonlinear vibrating problems the linear operator $\tilde{L}$ is chosen in the form [30]:

$$\tilde{L}(q) = \ddot{q} + \omega^2 q \tag{15}$$

where ω is the fundamental frequency. Then, the solution of the problem is expressed in a power series in p where $p \in [0,1]$ is an embedding parameter. Using the standard perturbation method, the nonlinear governing equation is divided into several consequent linear equations which can be used in order to find the most accurate solution of the system. Using Eq. (11) the homotopy equation can be constructed as:

$$\ddot{q} + \omega^2 q + p\left[\left(\gamma_1' - \omega^2\right)q + \gamma_2' q^2 + \gamma_3' q^3 + \gamma_4' q^4 + \gamma_0'\right] + \alpha_1 p(1-p)q = 0 \tag{16}$$

Assume that the solution can be expressed in a power series in p as follows

$$q = q_0 + pq_1 + p^2 q_2 + \ldots \tag{17}$$

As the embedding parameter p increases from 0 to 1, the solution of equation (16) varies from the chosen initial guess $q_0(\bar{\tau})$ to the solution $q(\bar{\tau})$ of the considered nonlinear equation. Substituting Eq. (17) into Eq. (16), and rearranging based on powers of p-terms yields:

$$p^0 : \ \ddot{q}_0(\bar{\tau}) + \omega^2 q_0(\bar{\tau}) = 0, \quad q_0(0) = A, \quad \dot{q}_0(0) = 0 \tag{18-a}$$

$$p^1 : \ \ddot{q}_1(\bar{\tau}) + \omega^2 q_1(\bar{\tau}) = \omega^2 q_0(\bar{\tau}) - \alpha_1 q_0(\bar{\tau}) - \left[\gamma_1' q_0(\bar{\tau}) + \gamma_2'\left(q_0(\bar{\tau})\right)^2 + \gamma_3'\left(q_0(\bar{\tau})\right)^3 + \gamma_4'\left(q_0(\bar{\tau})\right)^4 + \gamma_0'\right], \ q_1(0) = 0, \ \dot{q}_1(0) = 0 \tag{18-b}$$

$$p^2 : \ \ddot{q}_2(\bar{\tau}) + \omega^2 q_2(\bar{\tau}) = \omega^2 q_1(\bar{\tau}) - \alpha_1 q_1(\bar{\tau}) + \alpha_1 q_0(\bar{\tau}) - \left[\gamma_1' q_1(\bar{\tau}) + 2\gamma_2' q_0(\bar{\tau}) q_1(\bar{\tau}) + 3\gamma_3' q_0^2(\bar{\tau}) q_1(\bar{\tau}) + 4\gamma_4' q_0^3(\bar{\tau}) q_1(\bar{\tau})\right], \ q_2(0) = 0, \ \dot{q}_2(0) = 0 \tag{18-c}$$

Solving equation (18-a) gives the initial approximate solution as:

$$q_0(\bar{\tau}) = A\cos(\omega\bar{\tau}) \tag{19}$$

substituting $q_0(\bar{\tau})$ into the governing differential equation for $q_1(\bar{\tau})$ results into:

$$\ddot{q}_1 + \omega^2 q_1 + \left(\frac{3}{4}\gamma_3' A^3 + \gamma_1' A - A\omega^2 + \alpha_1 A\right)\cos(\omega\bar{\tau}) + \frac{1}{4}\gamma_3' A^3 \cos(3\omega\tau) + \left(\frac{1}{2}\gamma_4' A^4 + \frac{1}{2}\gamma_2' A^2\right)\cos(2\omega\bar{\tau}) + \frac{1}{8}\gamma_4' A^4 \cos(4\omega\bar{\tau}) + \frac{1}{2}\gamma_2' A^2 + \frac{3}{8}\gamma_4' A^4 + \gamma_0' = 0, \quad q_1(0) = 0, \ \dot{q}_1(0) = 0 \tag{20}$$

Eliminating the secular term leads to:

$$c_1(\omega, \alpha_1) = \frac{3}{4}\gamma_3' A^3 + \gamma_1' A - A\omega^2 + \alpha_1 A = 0 \tag{21}$$

The first-order approximate solution with assumption $\alpha_1 = 0$ is achieved as:

$$\omega = \sqrt{\gamma_1' + \frac{3}{4}\gamma_3' A^2} \tag{22}$$

In order to achieve the high accurate solution, the third part of the right hand side of equation (17) must be included. A special solution of equation (18-b) can be expressed as:

$$q_1(\bar{\tau}) = \frac{1}{6}\frac{A^2\left(\gamma_2' + \gamma_4' A^2\right)}{\omega^2}\cos(2\omega\bar{\tau}) - \frac{\gamma_3' A^3}{32\omega^2}\cos(3\omega\bar{\tau}) - \frac{\gamma_4' A^4}{120\omega^2}\cos(4\omega\bar{\tau}) - \frac{4\gamma_2' A^2 + 3\gamma_4' A^4 + 8\gamma_0'}{8\omega^2} \tag{23}$$

Using the perturbation method and substituting equation (23) leads to the third differential equation for $q_2(\bar{\tau})$. Solution of the third equation (18-c) should not contain the so-called secular term $\cos(\omega\bar{\tau})$. To ensure so, the coefficients of $\cos(\omega\bar{\tau})$ must be zero. Solving equation (21) for the parameter α_1 leads to:

$$\alpha_1 = \omega^2 - \frac{3}{4}\gamma_3' A^2 - \gamma_1' \tag{24}$$

Thereby, substituting this result together with equations (23) and (19) into the right hand side of equation (18-c) gives the secular term as:

$$c_2(\omega) = \gamma_1' A\omega^2 - 2A\gamma_2'\gamma_5' - \frac{7}{4}A^5\gamma_2'\gamma_4' + \frac{3}{4}A^3\gamma_3'\omega^2 - 3A^3\gamma_4'\gamma_5' - \frac{3}{128}A^5\gamma_3'^2 - \frac{191}{240}A^7\gamma_4'^2 - \frac{5}{6}A^3\gamma_2'^2 - \omega^4 A = 0 \tag{25}$$

Solving equation (25) for the fundamental frequency ω leads to:

$$\omega = \left(\frac{1}{2}\gamma_1' + \frac{3}{8}\gamma_3' A^2 + \left[\frac{1}{4}\gamma_1'^2 + \frac{3}{8}\gamma_3'\gamma_1' A^2 + \frac{15}{128}\gamma_3'^2 A^4 - 3\gamma_4'\gamma_5' A^2 - 2\gamma_2'\gamma_5' - \frac{7}{4}\gamma_2'\gamma_4' A^4 - \frac{5}{6}\gamma_2'^2 A^2 - \frac{191}{240}\gamma_4'^2 A^6\right]^{1/2}\right)^{1/2} \tag{26}$$

4. Results and discussion

The comparison between the results of numerical and analytical simulations have been illustrated in Fig. 3. Furthermore, to demonstrate the effectiveness of the second-order frequency amplitude relation, the asymptotic solutions using the first and second-order frequency relation described in equations (22) and (26) are also depicted in this figure. As clearly shown, the second-order approximation for $q(\bar{\tau})$ by employing equation (26) displays excellent agreement with numerical solutions using Runge-Kutta method. The influence of gradient index n on the pull-in behavior of vibrating FGM micro-cantilevers is depicted in Fig. 4. As can be seen, the fundamental frequency of the system decreases by increasing the initial condition A until the pull-in phenomenon occurs. In this situation, the frequency of oscillation drops to zero and the actuated micro-beam collapse onto the rigid plate. Fig.5 illustrates the fundamental frequency of micro-beam for some values of non-dimensional parameter μ_{1-2}. It is concluded that the fundamental frequency of micro-cantilever decreases as the parameter μ_{1-2} increases and pull-in instability happens at lower values of initial amplitude.

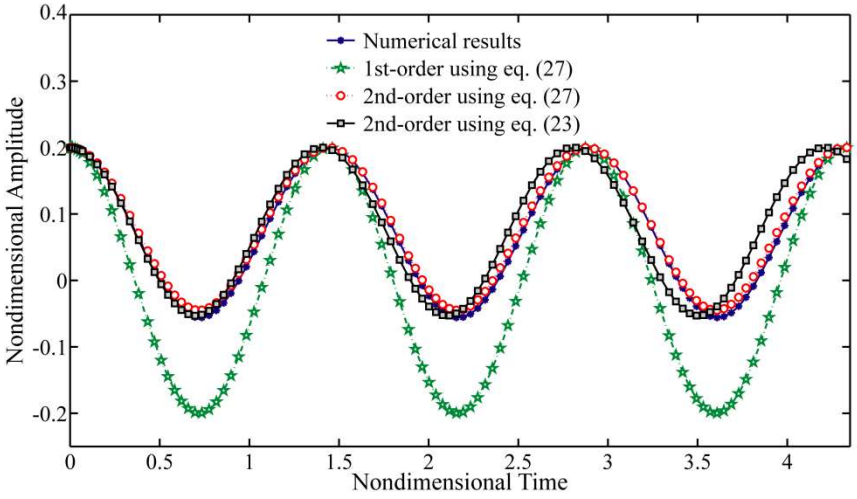

Fig. 3. Comparison of the results of analytical solutions with numerical solution for $A = 0.2,\ \gamma = 1, n = 0.25, \bar{V} = 2, \mu_{1-2} = 0.25$

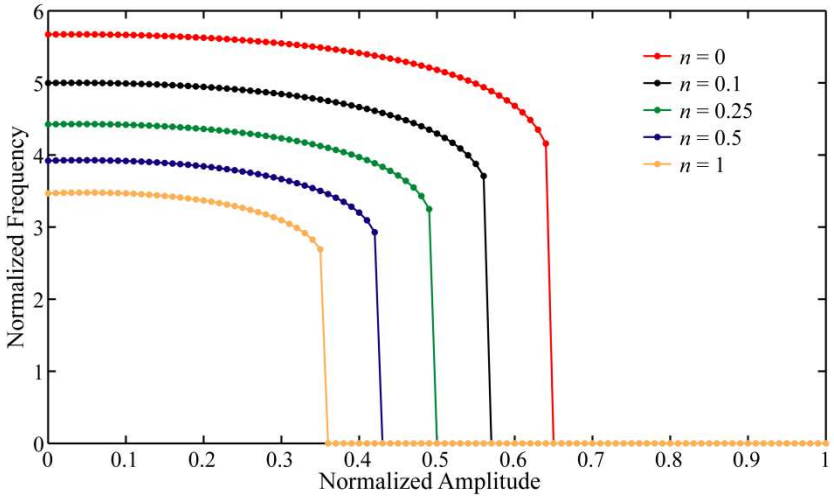

Fig. 4. Fundamental frequency vs. initial amplitude of micro-cantilever vibration, the effect of gradient index n

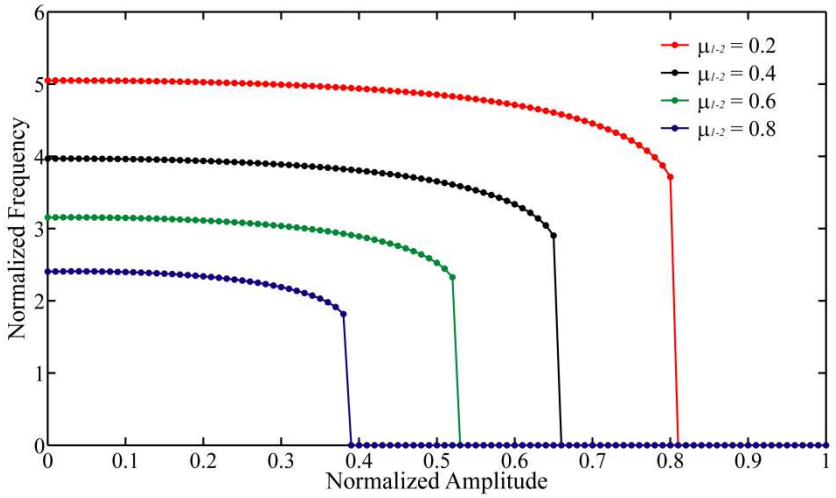

Fig. 5. Fundamental frequency vs. initial amplitude of micro-cantilever vibration, the effect of parameter μ_{1-2}

The influence of actuation voltage $\bar{V}$ on the fundamental frequency as a function of initial amplitude of vibration has been shown in Fig. 6. It is clearly exhibited that the fundamental frequency decreases as the parameter $\bar{V}$ increases and pull-in instability happens in the long domains of initial amplitude when the fundamental frequency of micro-beam drops to zero.

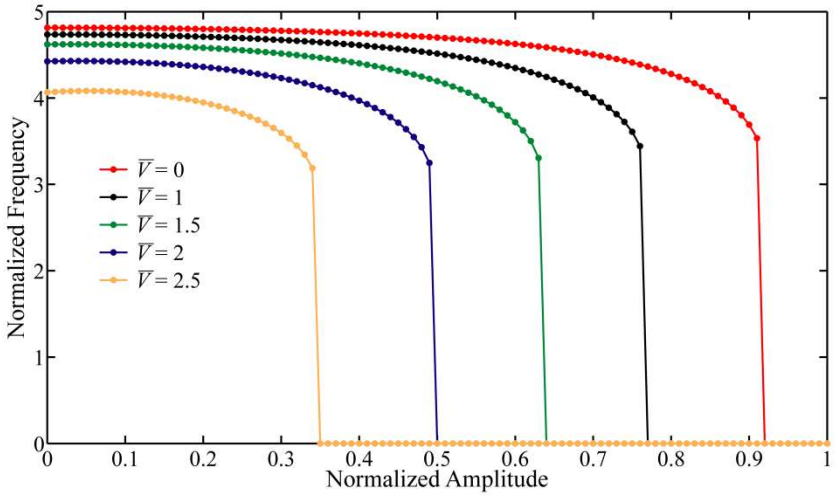

Fig. 6. Fundamental frequency vs. initial amplitude of micro-cantilever vibration, the effect of actuation parameter $\bar{V}$

The effect of fringing-field correction factor β_{es} on the dynamic pull-in behavior of actuated micro-beams is investigated in Fig. 7. It is obviously shown that the impact of the fringing-field is to reduce the pull-in voltage. In other words, when the fringing-field effect is taken into account, the pull-in phenomenon occurs at lower values of applied voltage. On the other hand, it can be observed that the dynamic pull-in voltage decreases by increasing the gradient index n. When the index n approaches to infinity, the variation of gradient index does not have any influence on the dynamic behavior of the system. Furthermore, it is concluded from Fig. 8 that with increasing the non-dimensional parameter μ_{1-2}, the dynamic pull-in voltage of the micro-cantilever decreases.

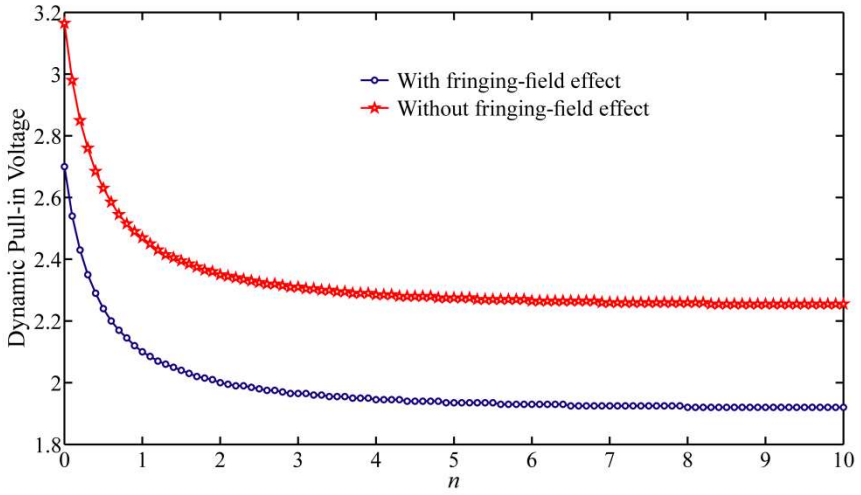

Fig 7. Dynamic pull-in voltage vs. gradient index n and the fringing-field correction factor β_{es} for $\gamma = 1,\ \mu_{1-2} = 0.4,\ A = 0.2$

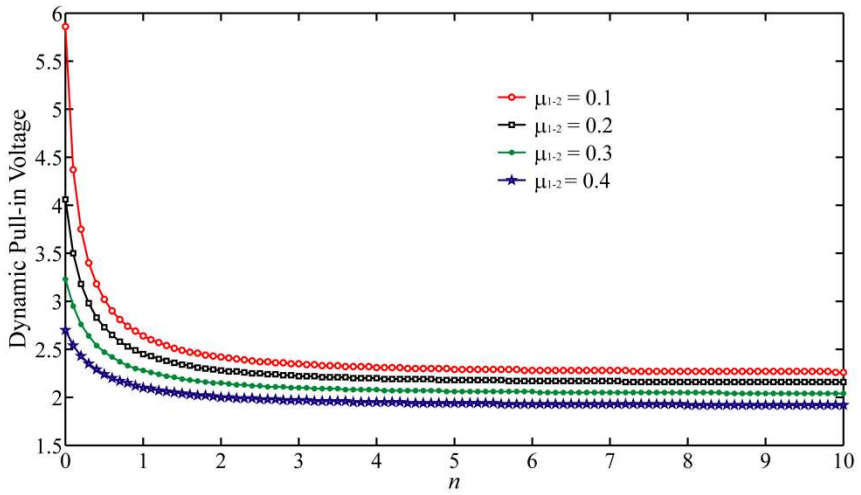

Fig 8. Dynamic pull-in voltage vs. gradient index n and the parameter μ_{1-2} for $\gamma = 1,\ A = 0.2$

5. Conclusion

As represented by this research, the dynamic pull-in behavior of FGM micro-cantilevers in the presence of fringing-field correction factor was investigated. It was indicated that with including the fringing-field effect included, the pull-in instability happens at lower values of applied voltage. Furthermore, the impact of material properties of functionally graded material parameters on the pull-in behavior was also studied. The illustrated results demonstrated that with increasing the gradient index of FGM materials, the dynamic pull-in voltage decreases. It was also exhibited that the auxiliary term in the homotopy perturbation method is extremely effective for higher order approximate solution and the second-order relation for the fundamental frequency using HPM with an auxiliary term has excellent agreement with numerical outcomes.

Acknowledgement

The author thanks National Iranian oil company (NIOC) and National Iranian South oil company (NISOC) for their help and financial support.

References

[1] Asghari, M., Ahmadian, M.T., Kahrobaiyan, M.H., Rahaeifard, M., "On the size-dependent behavior of functionally graded micro-beams", Materials and Design, Vol. 31, pp. 2324–2329, 2010.
[2] Lü, C.F., Chen, W.Q., Lim, C.W., "Elastic mechanical behavior of nano-scaled FGM films incorporating surface energies", Composites Science and Technology, Vol. 69, pp. 1124–1130, 2009.
[3] Craciunescu, C.M., Wuttig, M., "New ferromagnetic and functionally grade shape memory alloys", J Optoelectron Adv Mater, Vol. 5, No. 1, pp. 139–46, 2003.
[4] Fu, Y.Q., Du, H.J., Zhang, S., "Functionally graded TiN/TiNi shape memory alloy films", Mater Lett, Vol. 57, No. 20, pp. 2995–9, 2003.
[5] Fu, Y.Q., Du, H.J., "Huang WM, Zhang S, Hu M. TiNi-based thin films in MEMS applications: a review", Sensors Actuat A, Vol. 112, No. (2–3), pp. 395-408, 2004.
[6] Witvrouw, A., Mehta, A., "The use of functionally graded poly-SiGe layers for MEMS applications, Functionally Graded Mater, Vol. 8, pp. 255–60, 2005.
[7] Lee, Z., Ophus, C., Fischer, L.M., et al. "Metallic NEMS components fabricated from nanocomposite Al-Mo films", Nanotechnology, Vol. 17, No. 12, pp. 3063–70, 2006.
[8] Asghari, M., Rahaeifard, M., Kahrobaiyan, M.H., Ahmadian, M.T., "The modified couple stress functionally graded Timoshenko beam formulation", Materials and Design, Vol. 32, pp. 1435–1443, 2011.
[9] Jafar, I., Sadeghi-Pournaki, Zamanzadeh, M.R., Shabani, R., Rezazadeh, G., "Mechanical Behavior of a FGM Capacitive Micro-Beam Subjected to a Heat Source", Journal of Solid Mechanics, Vol. 3, No. 2, pp. 158-171, 2011.
[10] Ke, L.L., Wang, Y.S., "Size effect on dynamic stability of functionally graded microbeams based on a modified couple stress theory", Composite Structures, Vol. 93, pp. 342–350, 2011.
[11] Sharafkhani, N., Rezazadeh, G., Shabani, R., "Study of mechanical behavior of circular FGM micro-plates under nonlinear electrostatic and mechanical shock loadings", Acta Mech, Vol. 223, pp. 579–591, 2012.
[12] Das, K., Batra, R.C., "Pull-in and snap-through instabilities in transient deformations of microelectromechanical systems," J. Micromech. Microeng., Vol. 19, 035008, 2009. doi:10.1088/0960-1317/19/3/035008.
[13] Fu, Y., Zhang, J., "Size-dependent pull-in phenomena in electrically actuated nano beams incorporating surface energies," Applied Mathematical Modelling, Vol. 35, pp. 941-951, 2011.
[14] Wang, Y.G., Lin, W.H., Feng, Z.J., Li, X.M., "Characterization of extensional multi-layer microbeams in pull-in phenomenon and vibrations," International Journal of Mechanical Sciences, Vol. 54, pp. 225–233, 2012.
[15] Jia, X.L., Yang, J., Kitipornchai, S., "Pull-in instability of geometrically nonlinear micro-switches under electrostatic and Casimir forces," Acta Mech., Vol. 218, pp. 161-174, 2011. doi: 10.1007/s00707-010-0412-8.
[16] Sedighi, H.M., Shirazi, K.H., "Vibrations of micro-beams actuated by an electric field via Parameter Expansion Method," Acta Astronautica, Vol. 85, pp. 19-24, 2013.
[17] Rahaeifard, M., Ahmadian, M.T., Firoozbakhsh, K., "Size-dependent dynamic behavior of microcantilevers under suddenly applied DC voltage," Proc IMechE Part C: J Mechanical Engineering Science, DOI: 10.1177/0954406213490376.
[18] Rajabi, F., Ramezani, S., "A nonlinear microbeam model based on strain gradient elasticity theory," Acta Mechanica Solida Sinica,Vol. 26, No. 1, 2013, doi: 10.1016/S0894-9166(13)60003-8.
[19] Towfighian, S., Heppler, G.R., Abdel-Rahman, E.M., "Analysis of a Chaotic Electrostatic Micro-Oscillator," Journal of Computational and Nonlinear Dynamics, Vol. 6, No. 1, 011001, 2011.
[20] He, J.H., "Max-Min approach to nonlinear oscillators", International Journal of Nonlinear Sciences and Numerical Simulation, Vol. 9, pp. 207-210.
[21] Sedighi, H.M., Shirazi, K.H., Noghrehabadi, A., "Application of Recent Powerful Analytical Approaches on the Non-Linear Vibration of Cantilever Beams", Int. J. Nonlinear Sci. Numer. Simul., Vol. 13, No. 7–8, pp. 487–494, 2012.
[22] Ghadimi, M., Barari, A., Kaliji, H.D., Domairry, G., "Periodic solutions for highly nonlinear oscillation systems" Archives of Civil and Mechanical Engineering, Vol. 12, No. 3, pp. 389-395, 2012.
[23] Sedighi, H.M., Shirazi, K.H., Zare, J., "An analytic solution of transversal oscillation of quintic nonlinear beam with homotopy analysis method", International Journal of Non-Linear Mechanics, Vol. 47, pp. 777-784, 2012.
[24] Noghrehabadi, A., Ghalambaz, M., Ghanbarzadeh, A., "A new approach to the electrostatic pull-in instability of nanocantilever actuators using the ADM–Padé technique", Computers & Mathematics with Applications, Vol. 64, No. 9, pp. 2806–2815, 2012.
[25] Kaliji, H.D., Ghadimi, M., Pashaei, M.H., "Study the behavior of an electrically exciting nanotube using optimal homotopy asymptotic method", Int. J. Appl. Mechanics, Vol. 04, 1250004, 2012, DOI: 10.1142/S1758825112001336.
[26] Shou, D.H., He, J.H., "Application of parameter-expanding method to strongly nonlinear oscillators", International Journal of Nonlinear Sciences and Numerical Simulation, Vol. 8, No. (1), pp. 121-124, 2007.
[27] Sedighi, H.M., Shirazi, K.H., Noghrehabadi, A.R., Yildirim, A., "Asymptotic Investigation of Buckled Beam Nonlinear Vibration," Iranian Journal of Science and Technology, Transactions of Mechanical Engineering, Vol. 36, No. (M2), pp. 107-116, 2012.
[28] He, J. H., "Hamiltonian approach to nonlinear oscillators", Physics Letters A, Vol. 374, No. (23), pp. 2312-2314, 2010.

[29] Sedighi, H.M., Shirazi, K.H., Attarzadeh, M.A., "A study on the quintic nonlinear beam vibrations using asymptotic approximate approaches", Acta Astronautica, Vol. 91, pp. 245-250, 2013.
[30] He, J.H., "Homotopy Perturbation Method with an Auxiliary Term", Abstract and Applied Analysis, Vol. 2012, 857612, doi:10.1155/2012/857612.
[31] Batra, R.C., Porfiri, M., Spinello, D., "Vibrations of narrow microbeams predeformed by an electric field", Journal of Sound and Vibration, Vol. 309, pp. 600-612, 2008.
[32] He, J.H., "Homotopy perturbation method with two expanding parameters," Ind. J. Phys., Vol. 88, No. 2, pp. 193-196, 2014.

Appendix

$$\gamma_1 = -\bar{V}\left(2+\gamma\beta_{es}\right) \tag{A.1}$$

$$\gamma_2 = -\bar{V}\left(3+\delta\beta_{es}\right) \tag{A.2}$$

$$\gamma_3 = -\bar{V}\left(4+\gamma\beta_{es}\right) \tag{A.3}$$

$$\gamma_4 = -\bar{V}\left(5+\gamma\beta_{es}\right) \tag{A.4}$$

$$\gamma_0 = -\bar{V}\left(1+\gamma\beta_{es}\right) \tag{A.5}$$